Available online at www.sciencedirect.com
SCIENCE DIRECT®
Journal of Power Sources 122 (2003) 85–94
JOURNAL OF POWER SOURCES
www.elsevier.com/locate/jpowsour

Flooded utilization and electrochemical voltage spectroscopy studies on nickel electrodes

L.H. Thaller*, A.H. Zimmerman, G.A. To

The Aerospace Corporation, El Segundo, CA 90245, USA

Received 16 October 2002; accepted 16 November 2002

Abstract

A group of standard nickel electrodes were evaluated at different test temperatures and in different electrolyte concentrations. These production quality electrodes came from different backgrounds in terms of number of charge/discharge cycles, cycling temperature, electrolyte concentration, and cobalt level in the active material. The results of the matrix of tests using the flooded utilization (FU) technique demonstrated that capacity gains are available when cycling at lower temperatures and when higher concentrations of KOH are used as the electrolyte. Electrochemical voltage spectroscopy (EVS) scans were also taken for the complete matrix of tests. Since the cycling conditions used in the FU technique are much closer to those in actual cell cycling tests, they will be emphasized in this study in regard to the capacity trends. Comparative EVS scans were helpful in displaying the shifting potentials of the charging peaks of the active material relative to the oxygen evolution characteristics of these electrodes. The voltage span between the potential at which the active material is charged and the potential at which the co-evolution of oxygen becomes a significant parallel reaction determines the charging efficiency for the recharge step and is the root cause of the differences in useable electrode capacity.

Keywords: Electrochemical voltage spectroscopy; Flooded utilization; Nickel–hydrogen cells

1. Background

The amount of useable capacity at any point in time is an important parameter of nickel–hydrogen cells or batteries. A manufacturer is at liberty to assign a “nameplate” capacity value to a cell. Different manufacture have favored different KOH concentrations in their cells, different cobalt levels in their active material, and different cycling temperatures. Depending on the temperature at which the cell is charged and the end-of-charge voltage that is employed or the recharge ratio that is used, the cell may have a useable capacity that is higher or lower than its nameplate capacity. Since the ampere-hour (Ah) capacity of a nickel–hydrogen cell is related to the internal pressure, cells that are equipped with strain gauges can be monitored in terms of their capacity trends during the course of their cycling tests or their mission duration. A recent review of earlier Air Force- and NASA-sponsored cycling tests [1] revealed differences in the amounts of useable capacity as a function of cycling conditions and the concentration of KOH used as the electrolyte. Earlier phases of our laboratory studies [2,3] have shown the importance of the exact position of the charging characteristics of the active material relative to the oxygen evolution characteristics of the nickel electrode in determining the electrode’s useable capacity–charging efficiency relationship. Depending on the temperature range usually seen in cycling tests and orbital applications, the capacity of a cell towards the end of its useful life might vary by as much as 30–40% relative to other cells under test. To be best able to maximize the usefulness of these batteries in terms of their useable Ah capacities, these relationships and effects must be more fully understood. This further study represents an orderly review of the impact of different cell designs, electrode formulations, and electrolyte concentrations on the cycling characteristics of the active material. Earlier studies by other researchers have explored different aspects of this broad topic. NASA funded an extensive study of the effect of electrolyte concentration on the cycle life of nickel electrodes [4]. Comsat Laboratories studied the impact of cycling electrodes at different temperatures [5]. Earlier investigations within The Aerospace Corporation and elsewhere reviewed the impact of different additives on the chargeability of nickel electrodes [6,7]. The work to be described here will incorporate all of these effects within

* Corresponding author. Tel.: +1-310-336-6180; fax: +1-310-336-5846.
E-mail addresses: lawrence.h.thaller@aero.org (L.H. Thaller), albert.h.zimmerman@aero.org (A.H. Zimmerman).

0378-7753/03/$ – see front matter © 2003 The Aerospace Corporation. Published by Elsevier Science B.V. All rights reserved.
doi:10.1016/S0378-7753(02)00646-8

a large matrix of tests using samples of electrode material from the same parent electrode. Six different parent electrodes were selected for this study.

2. Introduction

The capacity that is available when discharging a nickel electrode depends on a number of factors. These include the loading level of active material impregnated into the porous nickel sinter, the average valence to which the active material is charged, and the amount of the active material that is participating in the charge/discharge process. The average valence at the end of the charging process is related to the end-of-charge voltage and/or the amount of overcharge that is charged back into the cell.

The useable Ah capacity of a nickel–hydrogen cell can also be viewed as depending on the amount of capacity that remains following that which has been lost due to various degradation mechanisms [8] and the amount that has been lost due to the capacity walkdown phenomenon [2,9]. In these references that addressed capacity walkdown, the impact of cycling temperature, electrolyte concentration, and number of accumulated cycles were investigated. The major finding of those studies determined the difference in potential between the potential at which the active material is charged to the higher capacity gamma-phase and the potential at which significant amounts of oxygen evolution takes place. This difference impacts the amount of useable Ah capacity that is available when the electrode is fully discharged as well as the charging efficiency during the charging process. The lower portion of Fig. 1 illustrates the position of the charging potentials for the beta- and gamma-phase materials relative to the potential at which oxygen is evolved at significant rates for one particular electrode. For a different electrode, one that has not been completely charged to the gamma-phase, the upper portions of Fig. 1 shows the potentials at which the beta- and gamma-phase portions of the active material are discharged. From these earlier studies, the positions of the different charging and discharging peaks were determined using the EVS technique at two different temperatures [3]. These results revealed that when cycled in 31% KOH, larger amounts of capacity are available when cycling at lower temperatures due to an increase in the separation of the potential at which the active material is charged to the gamma-phase and the potential at which significant amounts of oxygen are evolved in parallel with that reaction. It was also determined in this previous study that the charging potential of nickel hydroxide is higher when the supporting electrolyte is composed of 26% KOH as opposed to the more widely used 31% KOH. This results in a diminished separation between the charging potential for the active material and the potential where oxygen evolution becomes a significant factor in reducing the efficiency of the charging step. It would be expected to result in a reduced amount of useable Ah capacity in a cell using 26% KOH versus a similar cell using 31% KOH.

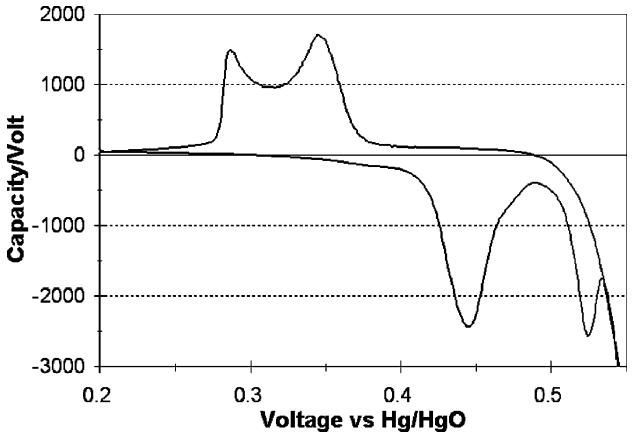

Fig. 1. Locating the beta and gamma charging and discharging peaks and the oxygen evolution characteristics of an electrode using the EVS technique.

Results from cycling tests on flight-weight nickel–hydrogen cells that compared the available capacities using these different KOH concentrations showed that at +10 °C, the cells activated with 31% KOH maintained a higher end-of-charge pressure compared with cells activated with 26% KOH [2]. When EVS and FU studies were carried out using 31% KOH, the results showed a clear capacity advantage when testing was carried out at −5 °C versus 24 °C for all electrodes tested [2]. The intent of this further study using samples of electrode material from the same set of six electrode used in the earlier study was to expand our understanding of their charging characteristics as impacted by several factors. These included the test temperature using 26% KOH as the electrolyte, the cobalt additive level in the active material, and the cycling history of the electrodes.

3. Description of the electrodes and tests

3.1. The electrodes

The electrodes used in these tests were standard, sintered nickel electrodes that had been removed from cells following life cycle testing or new electrodes that had not yet been installed into cells. These electrodes were selected based on coming from a wide variety of backgrounds in terms of cycling temperature, electrolyte concentration, number of accumulated charge/discharge cycles, and cobalt level in the active material. Table 1 summarizes the characteristics of the six sample electrodes. The ones that were removed from cells following cycling studies were still performing without any known performance problems. The sample sizes used in both the FU and the EVS studies were approximately 1.0 cm^2. Different samples from the same parent electrode were used for each FU or EVS test. Table 2

Table 1
Description of the electrodes used in the EVS and FU studies

Plate no.	No. of cycles	Approx. % Co	Cycling T (°C)	Electrolyte concentration, % KOH	Recharge ratio (%)
1	20	5	+20	31	Varied
2	40,000	5	+10	26	104
3	40,000	5	−5	26	103
4	40,000	10	+10	31	104
5	Not cycled	5	N.A.	N.A.	N.A.
6	Not cycled	10	N.A.	N.A.	N.A.

Table 2
Test matrix for the FU and EVS studies on the set of six different electrodes

Test temperature (°C)	Electrolyte concentration
−5	26 and 31% KOH
+10	26 and 31% KOH
+24	31% KOH

describes the matrix of tests that were carried out. All data were normalized to 1.0 cm^2 sample sizes.

3.2. Flooded utilization (FU) tests

The FU test was used to avoid electrolyte concentration effects that might be present in an actual operating cell. In this test, a nominal 1.0 cm^2 sample of electrode was placed in a container containing about 100 ml of electrolyte of the concentration to be used for the test. The potential of the electrode was measured relative to a Hg/HgO reference electrode. The container was placed in a constant temperature chamber held at the test temperature by a thick copper cold plate. A coolant fluid was circulated through a serpentine copper coil that was soldered to the bottom of the cold plate.

During the test, the electrode undergoes three successive charge/discharge cycles. The first cycle was used to convert the less active form of the active material into the more active form that is seen during normal charging and discharging of the active material [10]. Prior to the second charge cycle, the electrode was fully discharged in three-steps. During the first step, the electrode was discharged at the rate of 10 mA to a 1.0 V cutoff. This corresponds to about the C/4 rate if the electrode were in an actual nickel–hydrogen cell. The capacity at this rate is defined in these tests as the "useable capacity". Following this first step in the discharge process, the electrode was discharged further at the 2 mA rate to a −0.5 V cutoff. This capacity is referred to as the "residual capacity". The next step in the discharge was conducted at the 0.2 mA rate to a −0.5 V cutoff. This capacity is referred to as the "unavailable" capacity.

During the second cycle, the electrode was charged at approximately the C/10 rate for 10 h (4 mA). Following this charging step, the active material was still mostly in the beta-phase of the charged active material. Following the three-step discharge sequence, a third charging step was carried out. In this step, the C/10 charging rate is carried out for 14 h. This will charge different amounts of the active material to the gamma-phase. This form of the active material contains a larger amount of capacity since the average valance of the nickel ions in the gamma form is 3.66 as opposed to 3.0 for the beta-phase form of the active material. The amount of active material that is converted to the gamma-phase will depend on the charging potential of that material relative to the oxygen evolution characteristics of that electrode. Earlier studies with these same electrodes found that the position of the charging peaks relative to the oxygen evolution characteristics of each of these six electrodes was slightly different [2,3]. They depended on the cycling temperature, number of accumulated charge/discharge cycles, the electrolyte concentration, and cobalt level in the active material.

3.3. Electrochemical voltage spectroscopy (EVS) tests

EVS testing was carried out in parallel with the samples tested using the FU technique. The setup for this test was very similar to that used for the FU test. A nominal 1.0 cm^2 sample of electrode was immersed in a container containing about 100 ml of electrolyte of the concentration to be used in the test. Its potential was measured relative to a Hg/HgO reference electrode. The container was placed in a constant temperature chamber held at the test temperature by a thick copper cold plate. A coolant fluid was circulated through a serpentine copper coil that was soldered to the bottom of the cold plate. Unlike the charging and discharging step in the FU test, the voltage in the EVS test was increased or decreased much more slowly. In the tests to be described here, the voltage was changed at the rate of 2 μV/s. The test results are very similar to what would be obtained using the sweep voltammeter technique.

After a sample was placed in the test cell, the voltage was first decreased to 0.2 V to completely discharge all of the active material. Next, the voltage was increased at the rate of 2 μV/s to the end-of-charge voltage (in this case 0.56 V). The amount of charge that was consumed during the charging process is the integrated area under the curve. During the first charging scan, the active material was still in the less active form since the electrode had been at rest for a number of weeks [10]. As the charging voltage approaches 0.56 V, the electrode enters a region where oxygen evolution and charging of some of the active material occur in parallel. Upon reaching the end-of-charge voltage of 0.56 V, the voltage was reduced at the rate of 2 μV/s. Upon reaching about 0.35 V, the higher voltage beta material is first discharged, followed by the gamma-phase material at about 0.29 V. After again reaching 0.2 V, a second cycle was carried out. As seen in the Fig. 2, the charging of the active material to the beta-phase now occurs at a lower potential. Again, no distinct peak is seen for the charging of some of the material to the gamma-phase. However, during the discharge portion of

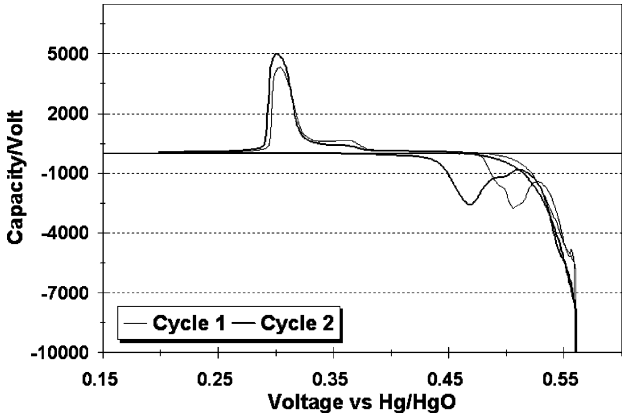

Fig. 2. Typical results from an EVS test using a first and second scan.

the sweep, a larger amount of gamma-phase material and a smaller amount of beta-phase material is seen. Earlier studies [3] on these same electrodes showed that, depending on the cycling temperature, KOH concentration, and cycling history, these charging and discharging peaks would move. During the −5 °C cycling tests in 31% KOH, distinct gamma charging peaks could be seen for all the plate samples. The electrolyte concentration used in the test shown in Fig. 2 was 26% KOH, and the cycling temperature was +10 °C.

4. Flooded utilization results

The useable capacity (*C*/4 to 1.0 V) values per cm^2 are shown for the set of six representative electrodes in Table 3. The amounts of useable capacity available are increased significantly at lower temperatures when using 31% KOH versus tests that were carried out at higher temperatures using 26% KOH. When the temperature was reduced to −5 °C, the capacity shortfalls associated with the use of 26% KOH were increased versus an expected reduction based on cycling results of flight-weight 50 Ah cells that had been life tested at the Navy Facility in Crane, IN under Air Force sponsorship [11]. Also to be noted are the capacity gains associated with some of the electrodes that had been cycled for 40,000 cycles (plates nos. 2–4) when the cycling temperature was reduced to −5 °C compared to lesser gains for the newer electrodes (plate nos. 1, 5, and 6). Table 4 compares these gains for two different experiments.

Table 3
Useable capacities for FU studies at the *C*/4 rate to a 1.0 V cutoff following a 14 h charge at about the *C*/10 rate (mAh/cm^2)

Plate no.	−5 °C, 31% KOH	−5 °C, 26% KOH	+24 °C, 31% KOH	+10 °C, 26% KOH
1	36.25	28.03	36.11	28.07
2	31.58	23.01	25.99	26.38
3	30.58	22.88	27.01	22.45
4	35.62	23.07	29.84	23.84
5	31.44	25.13	29.78	26.62
6	32.37	26.46	29.61	26.99

Table 4
Useable capacity gains available at a reduced temperature and an increased electrolyte concentration

Plate no.	% useable capacity gain −5 °C, 31% vs. +10 °C, 26%
1	29
2	19
3	36
4	56
5	18
6	20

Table 5
Capacities from Table 3 at the *C*/4 rate to a 1.0 V cutoff prorated to a 48-plate, 50 Ah nameplate cell (Ah)

2400 cm^2 cell	−5 °C, 31% KOH	−5 °C, 26% KOH	+24 °C, 31% KOH	+10 °C, 26% KOH
1	87	67	87	67
2	76	55	62	63
3	73	55	65	54
4	85	60	72	55
5	75	60	71	64
6	78	64	71	65

Table 5 projects the capacities following 14 h of charge at about the *C*/10 rate to a typical 48-plate, 3.5 in. cell with a nameplate capacity of 50 Ah. For comparison, a typical standard electrode might be 30 mil thick, 82% porous, 3.5 in. diameter, and loaded with 1.65 g of $Ni(OH)_2$ per cm^3 of void volume. The weight of active material in one of these electrodes would be 5.03 g. This is equivalent to 1.45 Ah per electrode, assuming a valance change of 1 and 2.43 Ah per electrode assuming a valance change of 1.67 (the amount required to charge up to the gamma-phase). The "theoretical" capacity of this cell when fully charged to the gamma-phase would be about 116 and 70 Ah assuming the cell would be only charged to the beta-phase.

5. Electrochemical voltage spectroscopy results

The EVS results can be presented in three different forms. The first is a chart depicting one or more sweeps as shown in Fig. 2. Another useful form of the results is a table listing the positions of the different charging and discharging peaks as a function of the cycling conditions. A third way of presenting the results is by integrating the area under the discharge portion of the sweep. Each of these forms has been found to be useful in making certain comparisons showing the difference in old versus new electrodes, cycling at −5 °C versus cycling at +10 °C, or cycling in 26% KOH versus cycling in 31% KOH. The capacity available during the discharge portion of an EVS sweep will be greater than a corresponding FU test since the charging and the discharge portions of

the cycle are carried out much more slowly. This permits both the charging step and discharge step to be carried out to a greater degree of completion.

5.1. Selected EVS scans

Fig. 3 compares the second EVS scan for two samples of the same electrode. One was scanned at room temperature and the other at −5 °C. Several features can be noted from this one figure. Most importantly, the voltage of the curve for oxygen evolution has shifted to a significantly higher potential. In doing so, a distinct gamma formation peak is now present. Compared with the scan at room temperature, the beta formation peak has receded to a slightly lower voltage, and the gamma peak has moved to a higher potential. At room temperature, the gamma peak appears only as a shoulder on the oxygen evolution curve. There does not appear to be a significant difference between the position of the gamma discharge peak at these two temperatures. In both of these experiments, all of the active material was charged to the gamma-phase as evidenced by the absence of a peak at or about 0.35 V. Based on the integrated area under the discharge curve, the total capacity obtained at room temperature appears to be higher than that obtained at the lower temperature. This was not the case in the FU tests that only counted the capacity at the *C*/4 rate to a 1.0 V cutoff. Fig. 4, similar to Fig. 2, compares the first and second scan of plate no. 1 that was cycled in 26% KOH at +10 °C. The charging peak for the beta material occurs at a significantly higher potential during the first scan compared with the second scan. There are no distinct gamma peaks during either scan although significant charging to the gamma-phase must take place in parallel with oxygen evolution since the discharge occurs primarily at the potential of the gamma material. Also to be noted is the larger amount of beta material during the first scan discharge due to the charging peak for the beta material being closer to the oxygen evolution curve during the first cycle. The relative narrowness of the beta charging peak during the first charge cycle suggests a greater degree of crystallinity of the material that had been at rest for many weeks compared the material during the second scan that was charged and discharged during the first cycle.

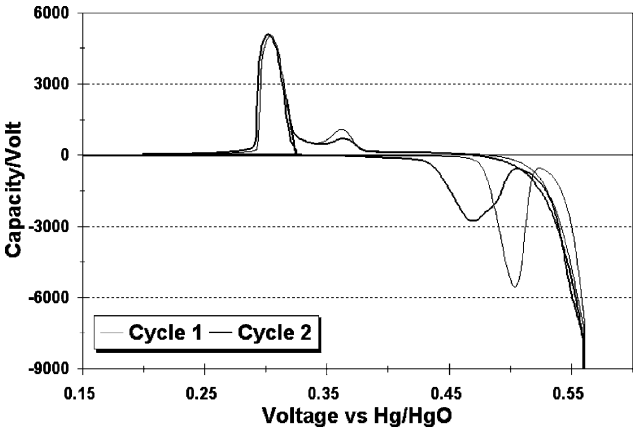

Fig. 4. Movement of the charge peaks between the first and second cycle.

Fig. 5 compares a typical plot for an electrode scanned at +10 °C in 26% KOH with one that was scanned at +10 °C in 31% KOH. Both of these electrodes were taken from plate no. 1. The main feature in this figure is the translation of the beta charging peak and gamma discharging peak to higher potentials in the case of 26% KOH. This is indicative of a higher charging voltage and a higher discharging voltage for cells filled with 26% KOH. This was found to be the case in the earlier studies of others [12]. It is also significant that there is an absence of any indication of a gamma charging peak in the case of the electrode scanned in 26% KOH. A distinct peak consistent with charging to the gamma-phase does appear in the case of the electrode scanned in 31% KOH.

Fig. 6 displays the impact of corrosion effects on the surface of the nickel sinter substrate following extended charge/discharge cycling. Plate 4 had undergone 40,000 successful charge/discharge cycles under conditions that resulted in about 22% corrosion of the nickel substrate [1]. This caused a buildup of non-cobalt-containing active ma-

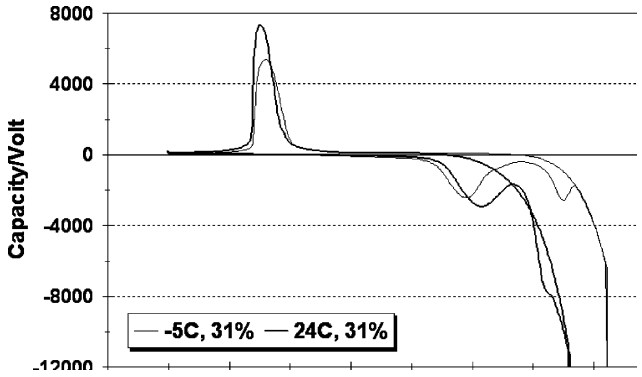

Fig. 3. The second EVS scan on samples from plate no. 4 at two different temperatures.

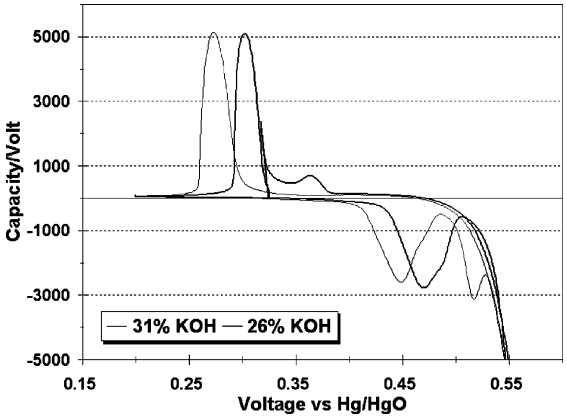

Fig. 5. EVS scans at +10 °C of samples tested in different electrolyte concentrations.

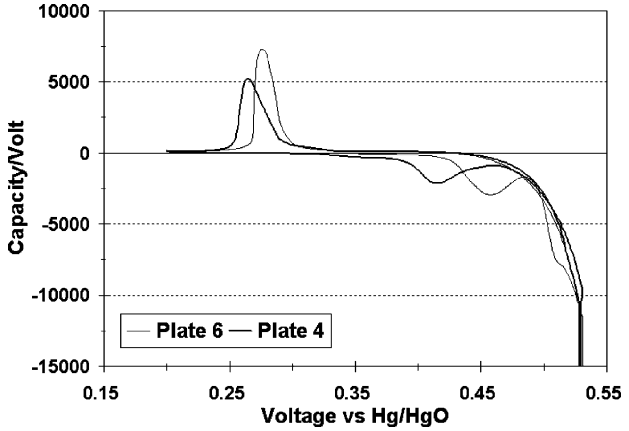

Fig. 6. Changes in the location of the beta charge peak following 40,000 cycles at +10 °C.

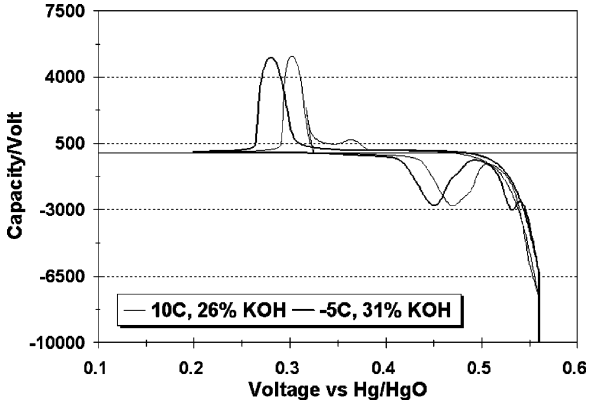

Fig. 7. Change in location of the charging and discharging peaks with change in KOH concentration and cycling temperature.

terial adjacent to the current collector. This had the effect of the active material at the surface of the current collector, acting as if it had a lower cobalt content. This resulted in requiring a higher charging voltage due to the shift in the charging characteristics of the active material. This gradual increase in the required charging voltage would result in a gradual reduction in charge efficiency or usable capacity over the course of life cycle testing or a satellite mission.

Fig. 7 compares the EVS scans from plate no. 1. This figure appears to be similar to Fig. 5 except the change in this figure is the temperature as well as the KOH concentration. As the temperature is lowered and the KOH concentration is increased, there is a shift to lower voltages for both charging peaks and the gamma discharge peak. This allows a greater span between where the active material is charged and where the co-evolution of oxygen becomes a concern relative to maintaining an acceptable charge efficiency and/or useable cell capacity.

5.2. Position of the charging and discharging peaks

In this subsection, the positions of the peaks appearing in some of the EVS scans that were generated as part of this study are tabulated. The values in the following tables will illustrate the movement in primarily the charging peaks of the beta and gamma materials as well as the oxygen generation characteristics. From these numbers the impact of new versus well-cycled electrodes, 26% KOH versus 31% KOH electrolytes, 5% cobalt additive versus 10% cobalt additive, cycled versus uncycled active material, as well as cycling temperature can be better understood.

Table 6 illustrates the difference in charging characteristics of active material that has remained in the uncharged state for several weeks compared with active material that has been recharged shortly after being discharged. This typical difference of about 35 mV; when prorated to a 21-cell battery, will amount to a difference in battery charging characteristics of about 0.75 V. This difference in potential is felt to be caused by the morphological differences between the structure of the active material after Ostwald ripening has occurred versus the less structured form of the active material that is continually charged and discharged. The charging voltage for the active material in plate nos. 4 and 6 (both started out with about 10% cobalt) changed over the course of cycling. After about 40,000 cycles on the cell from which plate no. 4 was taken, significant differences in the charging characteristics took place. The beta charging peak on the second scan of plate no. 6 is significantly lower than the

Table 6
Position of the beta and oxygen evolution characteristic during cycles one and two for the same set of six representative electrodes at +10 °C and 26% KOH, and the position of the gamma peak during discharge

Plate no.	First EVS cycle *E* vs. Hg/HgO reference electrode (V)	Second EVS cycle E vs. Hg/HgO reference electrode (V)	Difference from first cycle (mV)	Oxygen position (V)[a]	Second cycle gamma discharge peak (V)[b]
1	0.504	0.469	35	0.511	0.300
2	0.507	0.468	39	0.513	0.300
3	0.490	0.456	34	0.513	0.296
4	0.520	0.462	58	0.513	0.305
5	0.494	0.457	37	0.511	0.298
6	0.447	0.430	17	0.515	0.305

[a] The term oxygen position is the voltage at which the rate of oxygen evolution is significant relative to the conversion of active material to the gamma-phase. The selected rate of oxygen evolution was equal in all cases.

[b] There were no distinct gamma charging peaks associated with these electrodes.

Table 7
Position of the beta and oxygen evolution characteristic during cycle one and two for the same set of six representative electrode at −5 °C and 26% KOH, and the position of the gamma discharge peak

Plate no.	First EVS cycle E vs. Hg/HgO reference electrode (V)	Second EVS cycle E vs. Hg/HgO reference electrode (V)	Difference from first cycle (mV)	Oxygen position (V)[a]	Second cycle gamma discharge peak (V)[b]
1	0.516	0.492	24	0.532	0.309
2	0.517	0.475	42	0.531	0.306
3	0.511	0.476	35	0.532	0.310
4	0.534	0.496	38	0.529	0.309
5	0.498	0.483	19	0.524	0.307
6	0.453	0.429	24	0.531	0.310

[a] The term oxygen position is the voltage at which the rate of oxygen evolution is significant relative to the conversion of active material to the gamma-phase. The selected rate of oxygen evolution was equal in all cases.
[b] There were no distinct gamma charging peaks associated with these electrodes.

other five plates, signifying that a lower charging voltage is required for that type of electrode. Table 7 lists information similar to Table 6 except for tests carried out at −5 °C.

In Tables 8–10, the sets of electrodes, all using 31% KOH, were cycled at several different temperatures. Tables 8 and 9 first appeared in [3]. There was very little shift in the beta charging peaks between −5 and +24 °C. At the lower temperature, the gamma charging peaks moved to a higher voltage by about 20 mV. The oxygen evolution characteristic moved about 50 mV higher. This movement permitted a greater span between the charging of the active material to the gamma-phase and the co-evolution of oxygen. Apparently the kinetics of the oxygen evolution are reduced significantly as the temperature is lowered. This is the main factor in being able to obtain a larger amount of useable capacity at the lower temperature while maintaining an acceptably high round-trip efficiency.

The EVS scans shown in Fig. 2 were generated from a sample of electrode plate no. 2. The discharge peaks for both the beta material and the gamma material moved only about 5 mV from discharge scan 1 and discharge scan 2. Plate nos. 4 and 6 started with about 10% Co additive in the active material. After 40,000 cycles, the active material in plate no. 4 acts similarly to the electrodes that were made with 5% Co additive after it has cycled one time to convert the active material into the form that is more easily charged. The smaller the potential versus the reference electrode, the further away from oxygen evolution does the charging of the beta material take place. None of the six electrodes displayed a unique gamma charging peak when cycled at +10 °C and

Table 8
Position of the beta, gamma, and oxygen peaks during the second scan for the same set of six representative electrodes at +24 °C, and 31% KOH

Plate no.	Beta peak (V)	Gamma peak (V)	Oxygen position (V)	Gamma–beta[a] (V)	Gamma discharge peak (V)[b]
1	0.452	None	0.505	N.A.	0.277
2	0.457	0.51	0.505	0.053	0.277
3	0.450	None	0.505	N.A.	0.276
4	0.456	0.51	0.505	0.054	0.276
5	0.450	None	0.485	0.060	0.272
6	0.408	None	0.505	N.A.	0.262

[a] The value is the difference in the peak voltages for charging to the beta-phase and charging to the gamma-phase.
[b] The term oxygen position is the voltage at which the rate of oxygen evolution is significant relative to the conversion of active material to the gamma-phase. The selected rate of oxygen evolution was equal in all cases.

Table 9
Position of the beta, gamma and oxygen peaks during the second scan for the same set of six representative electrodes at +10 °C, and 31% KOH

Plate no.	Beta peak (V)	Gamma peak (V)	Oxygen level[a] (V)	Gamma–beta[b] (V)	Gamma discharge peak (V)
1	0.449	0.517	0.520	0.068	0.273
2	0.452	0.516	0.536	0.063	0.278
3	0.438	0.514	0.521	0.076	0.274
4	0.448	0.513	0.525	0.068	0.270
5	0.449	0.517	0.521	0.068	0.274
6	0.409	N.A.	0.524	N.A.	0.263

[a] The term oxygen position is the voltage at which the rate of oxygen evolution is significant relative to the conversion of active material to the gamma-phase. The selected rate of oxygen evolution was equal in all cases.
[b] The value is the difference in the peak voltages for charging to the beta-phase and charging to the gamma-phase.

Table 10
Position of the beta, gamma and oxygen peaks during the second scan for the same set of six representative electrodes at −5 °C, and 31% KOH

Plate no.	Beta peak (V)	Gamma peak (V)	Oxygen level[a] (V)	Gamma–beta[b] (V)	Gamma discharge peak (V)
1	0.451	0.532	0.545	0.081	0.278
2	0.450	0.527	0.550	0.077	0.279
3	0.442	0.530	0.550	0.088	0.276
4	0.445	0.525	0.540	0.080	0.278
5	0.442	0.528	0.545	0.086	0.279
6	0.412	None	0.550	N.A.	0.269

[a] The term oxygen position is the voltage at which the rate of oxygen evolution is significant relative to the conversion of active material to the gamma-phase. The selected rate of oxygen evolution was equal in all cases.
[b] The value is the difference in the peak voltages for charging to the beta-phase and charging to the gamma-phase.

Table 11
EVS capacities per cm^2 of the six different nickel electrodes cycled at different temperatures and different electrolyte concentrations

Plate no.	+10 °C, 26% KOH first cycle (mAh)	+10 °C, 26% KOH second cycle (mAh)	−5 °C, 31% KOH first cycle (mAh)	−5 °C, 31% KOH second cycle (mAh)
1	43.92	46.46	48.34	48.52
2	36.02	39.12	39.20	39.78
3	37.55	39.12	36.93	37.27
4	35.34	39.69	40.72	40.95
5	43.46	46.24	48.35	48.60
6	35.02	38.52	40.95	41.07

using 26% KOH. The charging of most of the active material to the gamma-phase took place concurrently with the evolution of oxygen.

5.3. Capacities under the discharge portion of the EVS scans

By integrating the areas in the negative portion of the scan, the number of mAh of charge involved with that portion of the scan can be calculated. The area under the positive portion of the scan represents the amount of capacity that is available following the charging portion of the scan. The charging efficiency can be determined once these two numbers are known. The charging efficiencies are purposely very low in these tests since the end-of-charge voltages were set as in Fig. 2, where oxygen evolution is the main reaction at the conclusion of the charging portion of the scan. As with the FU results in Table 3, there is a general trend toward higher capacities as the temperature is lowered and the KOH concentration is increased. Due to the more thorough charging process associated with the EVS technique, there is a smaller gain in capacity at the lower temperature compared with the FU results, as illustrated in Table 11.

The electrodes reported in Table 11 were charged to an end-of-charge voltage where essentially all the charging of the active material has taken place and only oxygen evolution occurs. Tables 12–14 illustrate the increase in capacity as determined by an EVS test as compared to the useable portion of capacity as measured in a FU test. The capacities from the EVS tests, as expected, were consistently higher by about 10–15%.

Table 12
Comparison of useable capacity from the 14 h FU test and the total capacity from the second EVS scan, both tests conducted at +10 °C

Plate no.	FU capacity (mAh)	EVS capacity (mAh)	Ratio FU/EVS
1	37.16	43.32	0.86
2	33.90	38.92	0.87
3	30.86	35.74	0.86
4	33.20	39.85	0.83
5	35.77	37.21	0.96
6	33.75	43.58	0.77

Table 13
Comparison of useable capacity from the 14 h FU test and the total capacity from the second EVS scan, both tests conducted at −5 °C

Plate no.	FU capacity with 31% KOH (mAh)	EVS capacity with 31% KOH (mAh)	Ratio FU/EVS
1	36.25	48.34	0.75
2	31.58	39.20	0.81
3	30.58	36.93	0.83
4	35.62	40.72	0.87
5	31.44	48.35	0.65
6	32.87	40.95	0.80

6. Summary

The different FU tests indicated the trends in useable capacity as a function of the different factors studied here. Locating the positions of the different charging peaks relative to the oxygen evolution characteristics provided reasons for these trends. The summary will relate these two

Table 14
Comparison of useable capacity from the 14 h FU test and the total capacity from the second EVS scan, both tests conducted at −5 °C

Plate no.	FU capacity with 26% KOH (mAh)	EVS capacity with 26% KOH (mAh)	Ratio FU/EVS
1	28.03	32.56	0.86
2	23.01	23.69	0.97
3	22.88	26.38	0.87
4	25.07	27.75	0.90
5	25.13	31.81	0.79
6	26.46	28.12	0.94

associated features for the different side-by-side comparisons. The relative position of the potential at which oxygen evolution becomes a significant parallel reaction as the active material is charged is common to all of these comparisons.

6.1. Cobalt concentrations of the active material

As the cobalt concentration in the active material is increased, the potentials at which the beta and gamma charging reactions occur are decreased relative to the potential at which the co-evolution of oxygen becomes a significant parallel reaction. This results in about a 20–30 mV decrease in both the charging and discharging voltage of cells using a cobalt additive level of about 10%. This will result in a higher amount of useable capacity and/or higher charging efficiencies. After many thousands of charge/discharge cycles, this advantage will decrease as the surface of the sinter substrate becomes depleted of the cobalt additive due to corrosion effects at the sinter/active material interface. By lowering the cycling temperature, the span between the charging reactions and oxygen evolution reaction will be increased due to the slower kinetics of the oxygen evolution reaction and the lower rates of sinter corrosion.

6.2. Electrolyte concentrations

The KOH concentration has a significant impact on the capacities measured using the FU and EVS techniques. The use of 26% KOH as the electrolyte concentration resulted in a reduction in the useable capacity at +10 °C as well as at −5 °C. This reduction in the FU as well as the EVS capacities occurred since the active materials containing both 5 and 10% cobalt additive have higher charging voltages when cycling in 26% KOH versus 31% KOH. That is, the charging voltages are closer to the oxygen evolution voltage when cycled in 26% KOH. By reducing the cycling temperature, the reduction in capacity versus the values obtained with 31% KOH are increased significantly for both the FU tests and the EVS tests.

6.3. Cycling temperatures

Cycling at the reduced temperature of −5 °C versus +10 °C resulted in an increase in useable capacity in the case of EVS tests as well as in the case of the FU tests when 31% KOH was used as the electrolyte. Cycling temperature has this significant impact on the useable capacity since the kinetics of the oxygen evolution reaction are reduced significantly in the case of 31% KOH electrolytes. This creates an increased span between the charging potential of the active material and oxygen evolution. This occurs even though the charging potentials for both the beta and gamma reactions are increased as the temperature is lowered. In the case of 26% KOH, there was a significant reduction in the FU and EVS capacities at the lower temperature. In part, this was caused by a decrease in the span between the charging of the active material resulting in an increase in the rate of oxygen evolution.

6.4. Well-cycled versus uncycled electrodes

As electrodes are cycled, there is a gradual loss in the useable capacity due to the buildup of non-cobalt-containing active material on the surface of the nickel sinter substrate. This build-up causes the electrode to behave like one that contains a lesser amount of cobalt additive. This results in an increase in the potential required to charge the active material. In doing so, a reduced charging efficiency or a reduction in the useable capacity will occur since there is an increase in the amount of oxygen generated in parallel with the charging reaction.

6.5. Activated versus inactive forms of active material

Nickel hydroxide that has remained uncycled for an extended period of time is believed to recrystallize into larger crystallographic entities. These larger crystals have higher reversible potentials. This increase in charging potential (20–40 mV) results in a reduced charging efficiency when an attempt is made to bring the cell back to full useable capacity. In a nickel–hydrogen cell, this is evidenced when attempting to charge a cell to full capacity after some of the active material has been allowed to remain in the discharged state for an extended period of time.

Acknowledgements

The life cycle data used in this report was made available from the data basing programs sponsored by the Air Force and NASA. The tests themselves were carried out at the Navy Facility located at Crane, IN. Mr. Ralph James of the Air Force Research Laboratory in Albuquerque, NM, was instrumental in authorizing access to the day-to-day cycling data that was collected and stored at the Navy Testing Facility. Mr. Thomas Miller of the NASA Glenn Research Center in Cleveland, OH was helpful in facilitating access to the NASA-funded cycling database information that was also collected and stored at the Navy Facility. The Aerospace

Corporation is gratefully acknowledged for supporting this work as part of the Aerospace IR&D program.

References

[1] L.H. Thaller, A.H. Zimmerman, A Critical Review of Nickel–Hydrogen Life Testing, Aerospace Report No. ATR-2001 (8466)-2, May 2001.
[2] L.H. Thaller, A.H. Zimmerman, G.A. To, in: Proceedings of the 37th Intersociety Energy Conversion Engineering Conference on Understanding and Managing Capacity Walkdown in Nickel–Hydrogen Cells and Batteries, Washington, DC, 29 July–2 August 2002.
[3] L.H. Thaller, A.H. Zimmerman, G. To, A techniques to improve the usability of nickel–hydrogen cells, J. Power Sources 114 (2) (2003) 309–319.
[4] H.S. Lim, S.A. Verzwyvelt, in: Proceedings of the 20th IECEC on KOH Concentration Effect on the Cycle Life of Nickel–Hydrogen Cells, vol. 1, Miami Beach, 18–23 August 1985, pp. 165–170.
[5] H. Vaidanathan, et al., in: Proceedings of the 34th IECEC on Dependence of Positive Plate Design and Temperature on the Performance of Nickel–Hydrogen Cells, Paper 1999-01-2594, Vancouver, British Columbia, Canada, 2–5 August 1999.
[6] A.H. Zimmerman, P.K. Effa, in: Proceedings of 14th International Power Sources Symposium on the Effects of Additives on Nickel Electrode Discharge Kinetics, Brighton, England, September 1984, pp. 407–422.
[7] K. Watanabe, et al., Effect of cobalt addition to nickel hydroxide as a positive material for rechargeable alkaline batteries, J. Power Sources 58 (1996) 23–28.
[8] L.H. Thaller, in: Proceedings of the Sixth European Space Power Conference on Dealing with Capacity Loss Mechanisms in Nickel–Hydrogen Cells and Batteries, SP-502, Porto, Portugal, 6–10 May 2002.
[9] L.H. Thaller, A.H. Zimmerman, G.A. To, Capacity Management and Walkdown During LEO Cycling of Nickel–Hydrogen Cells and Batteries, Aerospace Report No. TR-2001(3310)-1, October 2000.
[10] L.H. Thaller, A.H. Zimmerman, in: Proceedings of the Fifteenth Annual Battery Conference on Applications and Advances on Electrochemical Voltage Spectroscopy for Analysis of Nickel Electrodes, Long Beach, CA, 11–14 January 2000, pp. 165–173.
[11] B.A. Moore, H.M. Brown, C.A. Hill, in: Proceedings of the 32nd IECEC on Air Force Nickel–Hydrogen Testing at NAVSURFWARCENDIV Crane, Honolulu, HA, 27 July–1 August 1997, pp. 186–191.
[12] J.D., Dunlop, G.M. Rao, T.Y. Yi, NASA Handbook for Nickel–Hydrogen Batteries, NASA Reference Publication 1314, 1993, pp. 5–21.